

Expression of Adrenergic and Cholinergic Receptors in Murine Renal Intercalated Cells

Jin-Gon JUN¹⁾, Seishi MAEDA^{1)*}, Sachi KUWAHARA-OTANI¹⁾, Koichi TANAKA¹⁾, Tetsu HAYAKAWA¹⁾ and Makoto SEKI¹⁾

¹⁾*Department of Anatomy and Cell Biology, Hyogo College of Medicine, 1-1 Mukogowa, Nishinomiya, Hyogo 663-8501, Japan*

(Received 18 June 2014/Accepted 11 July 2014/Published online in J-STAGE 28 July 2014)

ABSTRACT. Neurons influence renal function and help to regulate fluid homeostasis, blood pressure and ion excretion. Intercalated cells (ICCs) are distributed throughout the renal collecting ducts and help regulate acid/base equilibration. Because ICCs are located among principal cells, it has been difficult to determine the effects that efferent nerve fibers have on this cell population. In this study, we examined the expression of neurotransmitter receptors on the murine renal epithelial M-1 cell line. We found that M-1 cells express $\alpha 2$ and $\beta 2$ adrenergic receptor mRNA and the $\beta 2$ receptor protein. Further, $\beta 2$ receptor-positive cells in the murine cortical collecting ducts also express AQP6, indicating that these cells are ICCs. M-1 cells were found to express m1, m4 and m5 muscarinic receptor mRNAs and the m1 receptor protein. Cells in the collecting ducts also express the m1 receptor protein, and some m1-positive cells express AQP6. Acetylcholinesterase was detected in cortical collecting duct cells. Interestingly, acetylcholinesterase-positive cells neighbored AQP6-positive cells, suggesting that principal cells may regulate the availability of acetylcholine. In conclusion, our data suggest that ICCs in murine renal collecting ducts may be regulated by the adrenergic and cholinergic systems.

KEY WORDS: autonomic nervous system, nephrology, parasympathetic, renal epithelium, sympathetic

doi: 10.1292/jvms.14-0315; *J. Vet. Med. Sci.* 76(11): 1493–1500, 2014

Renal function is regulated, in part, by both humoral and neuronal factors. It has been postulated that neuronal factors may be less important than humoral factors in regulating renal function, given the fact that patients receiving kidney transplants, which have a defective renal plexus, maintain relatively normal renal function. However, the renal nervous system has been shown to be important in blood pressure regulation. For example, renal nerve ablation decreases blood pressure in both humans and animals [16, 36, 42, 44], and repression of circadian effects on blood pressure has been observed in renal transplant patients [13, 20]. Classical studies have shown that introduction of cholinergic agents into the renal artery causes hypotensive effects in mammals [9, 10, 46]. Barajas *et al.* found histological evidence of nephritic and vascular innervation in mammals and demonstrated an effect of this innervation on renal functions [3–7, 26]. However, the specific cellular targets of renal innervation remain unclear.

Previous reports have demonstrated sympathetic and parasympathetic effects on glomeruli, proximal tubules and collecting ducts [15, 24, 25, 28, 32, 35], but the specific effects on each cell type remain unknown. Several types of adrenergic receptors (ADRs) have been identified in the kidney. A range of ADR $\alpha 1$ and $\alpha 2$ subtypes is expressed by the renal

vasculature and by nephrons. Stimulation of these receptors causes arterial vasoconstriction and tubular reabsorption [21, 31, 40]. The ADR β subtypes are expressed by renin-secreting granule cells and by the proximal tubules [15, 41]. The muscarinic acetylcholine (ACh) receptors (mAChRs) are also expressed in cells within the glomeruli, proximal tubules and collecting duct [24, 25, 28, 32, 35] where they activate renal solute transport [32, 35]. It has been suggested that other renal cell types may express neurotransmitter receptors, but such expression patterns have yet to be defined.

Principal cells within the renal collecting ducts help to regulate urine concentration. Principal cells are segment-specific cells that are interspersed with intercalated cells (ICCs) in the renal epithelium. One of the major functions of principal cells is to reabsorb water through the arginine-vasopressin (AVP)-sensitive water channel, aquaporin 2 (AQP2) [27, 43]. Similarly, ICCs play a role in acid/base regulation by modulating proton conductance. ICCs can be distinguished by the expression of AQP6. AQP6 is a member of the aquaporin family that is localized to intracellular vesicles and is permeable to both water and anions [27, 43]. ICCs are classified into three types (A, B and non-A non-B) based on the expressions and intracellular localization of proton pumps and anion exchangers [19]. In the kidney, acid/base equilibrium is primarily regulated by the proximal tubules and collecting ducts [14]. The regulation of acid/base balance in proximal tubular cells can be affected by the cholinergic agent carbachol, suggesting some measure of neuronal influence [32, 35]. ICCs co-express AQP6 and the proton pump H^+ -ATPase on intracellular vesicles. These 2 molecules may act together to control acid/base balance within the body [30, 49]. Because ICCs are interspersed

*CORRESPONDENCE TO: MAEDA, S., Department of Anatomy and Cell Biology, Hyogo College of Medicine, 1-1 Mukogowa, Nishinomiya, Hyogo 663-8501, Japan. e-mail: maedas@hyo-med.ac.jp
©2014 The Japanese Society of Veterinary Science

This is an open-access article distributed under the terms of the Creative Commons Attribution Non-Commercial No Derivatives (by-nc-nd) License <<http://creativecommons.org/licenses/by-nc-nd/3.0/>>.

Table 1. List of aquaporin and neurotransmitter receptor primers

Gene	Subtype	Gene name	Upper primer 5'- to -3'	Lower primer 5'- to -3'	Size (bp)	Accession No.
Aquaporins	AQP2	<i>Aqp2</i>	ggggccacatcaacctge	agagcattgacagccagtc	172	BC019966
	AQP6	<i>Aqp6</i>	actggctgtccatgaacc	aggaaagtggccaggaggtac	206	BC115586.1
Adrenaline receptors	α 1	<i>Adra1a</i>	aatgcttctgaaggctccaa	tccagatctcaaatgatgg	252	BC113139.1
	α 2	<i>Adra2b</i>	ctggcctcgacctactaag	cacctcaaccacttccagt	278	BC156761.1
	β 2	<i>Adrb2</i>	aagaataaggcccagtggt	gtcttgaggctttgtgctc	383	BC032883.1
	β 3	<i>Adrb3</i>	actcctcgtaatgcc acc ag	gctgggtaagtctgtcagc	389	BC132000.1
Muscarinic acetylcholine receptors	m1	<i>Chrm1</i>	tactggcgcatctaccggga	gagaaggtctttcttggc	447	BC094242.1
	m3	<i>Chrm3</i>	cacggcagactctaactgatggggag	ttcaccaccaagactggaagcccagt	363	BC129893.1
	m4	<i>Chrm4</i>	gatggtgttcattcgacag	gcagaatagcgggtcaaagc	307	X63473.1
	m5	<i>Chrm5</i>	caggcctcctggtcatcctccttaga	taccaccaatcggaaacttataggcaac	355	BC120615.1
Glyceraldehyde-3-phosphate dehydrogenase		<i>Gapdh</i>	tgaaggtcgtgtgaaccgatttggc	catgtaggcatgaggtccaccac	982	M32599.1

within the collecting duct epithelium, it has been difficult to determine the specific effect of neuronal input on the ability of these cells to regulate the pH of body fluid.

The M-1 cell line consists of immortalized mouse renal epithelial cells. M-1 cells express H⁺-ATPase and several anion transporters that are expressed by renal ICCs [37, 38]. To determine if M-1 cells are a useful model with which to investigate the effects of neurotransmitters on ICCs, we examined M-1 expression of the ADR and mAChR neurotransmitter receptors and the expression and location of these receptors in murine ICCs.

MATERIALS AND METHODS

Cell culture: The M-1 mouse kidney epithelial cell line was obtained from DS Pharma Biomedical Co., Ltd. (Osaka, Japan). Cells were incubated in DMEM/Ham's F12 (1:1 mixture, Wako, Osaka, Japan) supplemented with 2 mM L-glutamine, 5% fetal bovine serum (Nichirei Biosciences, Tokyo, Japan) and 5 μ M dexamethasone (Sigma-Aldrich, St. Louis, MO, U.S.A.) at 37°C in a humidified atmosphere of 5% CO₂ and 95% air.

Animals: Adult male C57BL/6J mice (7 weeks old, 20–25 g) were obtained from Crea Japan, Inc. (Tokyo, Japan) and used according to protocols approved by The Animal Care and Use Committee at Hyogo College of Medicine. Mice were kept in separate cages and maintained under a 12-hr light/dark cycle at a constant temperature of 25°C. Food and water were given *ad libitum* until sacrifice.

Reverse transcription (RT)-PCR: Cultured cells (10–50 \times 10⁶ cells/ml) and murine kidneys (0.1 mg/ml) were homogenized with Trizol reagent (Invitrogen, Carlsbad, CA, U.S.A.), and total RNA was obtained according to the manufacturer's protocol. Genomic DNA was eliminated by incubating the samples with RNase free DNase I (Takara, Otsu, Japan). cDNA was synthesized with oligo dT and RTase (Toyobo, Osaka, Japan) from 2 μ g of total RNA. PCR was performed with ExTaqTM Hot Start version (Takara) with primers specific for the ADR subtypes, the mAChR subtypes, the aquaporins and the glyceraldehyde-3-phosphate dehydrogenase (GAPDH) (Table 1). PCR conditions were

as follows: hot start initiation at 94°C for 1 min followed by 35 cycles of 94°C for 30 sec, 60 or 64°C for 30 sec and 72°C for 30 sec, and ending with an additional extension reaction at 72°C for 10 min. In the GAPDH, PCR was performed with 20 cycles. PCR products were electrophoresed in 1.5% agarose gels and visualized with ethidium bromide and UV transillumination (ATTO, Tokyo, Japan). Negative control examination was performed with the same procedure, except for the omitting of RTase. To confirm whether the amplicons are normal in M-1 cell genome, PCR was also carried out with genomic DNA as templates.

Immunoblot: Confirmation of the expressions of ICC cellular markers and neurotransmitter receptors was performed by immunoblot. Normal murine kidney tissue and M-1 cells (5 \times 10⁶ cells/test) were homogenized, and then, total membrane proteins were purified by MinuteTM Plasma Membrane Protein Isolation kit (Invent, Eden Prairie, MN, U.S.A.). The total protein fraction was collected and denatured in 125 mM Tris-HCl (pH 7.6) containing 4% SDS, 1mM EDTA, 0.1 M dithiothreitol, 20% glycerol and 0.005% bromophenol blue at 4°C overnight. Samples were electrically separated in a urea denaturation polyacrylamide gel (10% polyacrylamide, 4 M urea). Separated proteins were transferred to polyvinylidene difluoride membrane at 1.5 mA/cm² for 50 min by semidry blotter (#EPE103AA, Advantech, Tokyo, Japan). Protein-transferred membranes were washed with phosphate buffered saline containing 0.05% Tween 20 (PBST) and blocked with Block AceTM (DS Pharma Biomedical) containing 0.5% normal goat serum (Vector, Burlingame, CA, U.S.A.). Membranes were incubated with diluted primary antibodies including rabbit anti-AQP6 polyclonal antibody (pAb, #AQP-006, Alomone Labs, Jerusalem, Israel), rabbit anti-AQP2 pAb (#AQP-002, Alomone labs), rabbit anti-ADR b2 pAb (#Sc-569, Santa Cruz, TX, U.S.A.) and rabbit anti-mAChR m1 pAb (#010, Alomone Labs) for 2 hr at room temperature or at 4°C overnight. After washing with PBST, membranes were incubated with diluted horseradish peroxidase-conjugated goat anti-rabbit IgG (Millipore, Billerica, MA, U.S.A.) for 2 hr at room temperature. Signal detection was carried out with chemi-luminescence ECLTM prime (GE Healthcare, Little Chalfont, U.K.) and a luminescent image

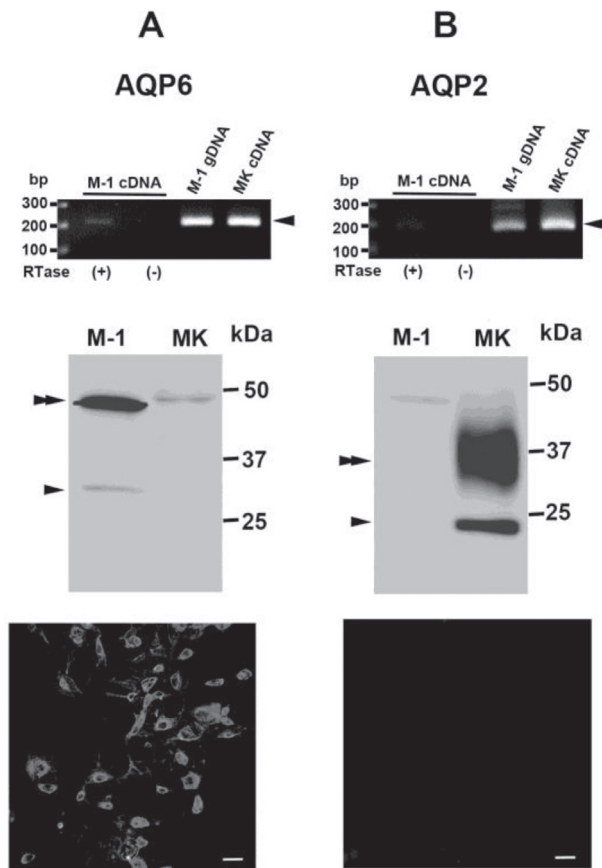


Fig. 1. Characterization of M-1 cellular expression of aquaporin. A) Characterization of AQP6 mRNA and protein expression in M-1 cells by RT-PCR (upper column) and immunoblot (middle column), respectively. An AQP6 specific band (arrowhead) was amplified from M-1 cellular total RNA (lane 1), M-1 cellular genomic DNA (gDNA, lane 3) and normal mouse kidney total RNA (MK cDNA, lane 4). No positive band was observed in RTase (-) negative control lane (lane 2). Immunoblot demonstrating the AQP6 specific band (arrowhead) and glycosylated band (double arrowhead) in total membrane protein extracted from M-1 cells (lane 1) and murine kidney (MK, lane 2). B) Characterization of AQP2 mRNA and protein expression in M-1 cells by RT-PCR (upper column) and immunoblot (middle column), respectively. AQP2 mRNA was not amplified from M-1 cellular total RNA (lane 1), although it was observed in M-1 gDNA (lane 3) and MK cDNA (lane 4). Similarly, AQP2 protein was not observed in total membrane protein isolated from M-1 cells (lane 1), although it was observed in total membrane protein isolated from the MK (lane 2). An arrowhead and a double arrow indicate the unglycosylated and glycosylated bands, respectively. Immunofluorescence showed the M-1 cells were positive to the AQP6 antibody (A, lower column), but negative to AQP2 antibody (B, lower column). Bar=50 μ m.

analyzer LAS-4010 (GE Healthcare). Control experiments were performed with primary antibodies pre-incubated with protein-specific blocking peptides.

Immunofluorescence of M-1 cells: To characterize the M-1 cells with expression of AQPs, the immunofluorescence was carried out by using anti-AQP2 and AQP6 antibodies. M-1

cells were cultured under the condition mentioned above in the 4-well slide chambers (Thermo Fischer Scientific, Waltham, MA, U.S.A.). Cells were fixed with 4% paraformaldehyde in PB for 10 min at room temperature. After washing with PBST, they were blocked with 10% normal goat serum in PBST, followed by incubation with primary antibodies (AQP2: #AQP-002; AQP6: #AQP-006, Alomone Labs) for 1 hr. After washing with PBST, they were incubated with rhodamine-conjugated goat anti-rabbit IgG pAb (Millipore). Light and fluorescent microscopic observations were obtained using a BX-51 (Olympus, Tokyo, Japan), and data were imported from a DP-73 CCD camera (Olympus).

Immunohistochemistry of the neurotransmitters on the renal tissues: Animals were anesthetized with medetomidine (0.3 mg/kg), midazolam (4 mg/kg) and butorphanol (5 mg/kg). Anesthetized animals were intracardially perfused with normal saline, followed by Zamboni's fixative. Kidneys were removed, dissected into small sections and then additionally fixed in Zamboni's fixative at 4°C overnight. Specimens were immersed in phosphate buffer (pH 7.4) containing graded sucrose (10–20%) and quickly frozen at -80°C. Tissues were sliced into 7 μ m sections by cryostat (Leica, Wetzlar, Germany), transferred to glass slides and air-dried. Before immunostaining, antigen retrieval was performed by submerging sections in 1 mM EDTA in Tris-HCl (pH 8.0) for 5 min at 115°C. Immunohistochemical staining was performed with the avidin-biotin complex (ABC) system. Tissue sections were submerged in 0.3% H₂O₂ in methanol for 30 min to eliminate endogenous peroxidases. Sections were then blocked with ABC blocking reagent (Vector) followed by 10% normal goat serum in PBST and incubated with rabbit anti-ADR β 2 pAb (#SC-569) or rabbit anti-mAChR m1 pAb (#010). After washing with PBST, sections were incubated with biotin-conjugated goat anti-rabbit IgG pAb (Millipore), and the ABC reaction was performed (ABC Elite, Vector). The sections were washed with PBST and then incubated in 0.04% diaminobenzidine containing 0.3% nickel ammonium and 0.003% H₂O₂ (DAB-Ni, Vector) for 10 min. After visualization under the microscope, sections were washed twice with 0.1 M glycine buffer (pH 2.5) for 5 min. After neutralization with PBST, sections were re-immunostained with the AQP6 antibody for cell-type identification. In brief, specimens were blocked with 10% normal goat serum in PBST and then incubated with rabbit anti-AQP6 pAb (#AQP-006). After washing with PBST, sections were incubated with rhodamine-conjugated goat anti-rabbit IgG pAb (Millipore). Light and fluorescent microscopic observations were obtained using a BX-51, and data were imported from a DP-73 CCD camera.

Acetylcholine (AChE) staining: Histochemistry of AChE in murine kidney slices was performed by the modified Karnovsky-Roots method [45]. Murine renal tissues were sliced into 7 μ m sections on a cryostat and transferred to glass slides. Specimens were washed in 0.1 M maleate buffer (pH 6.0) and then incubated in reaction buffer containing 36 μ M acetylthiocholine iodide, 5 μ M hexacyano-ferricite, 30 μ M copper sulfate and 50 μ M sodium citrate in 0.1 M maleate buffer (pH 6.0) for 30 min at room temperature. Sec-

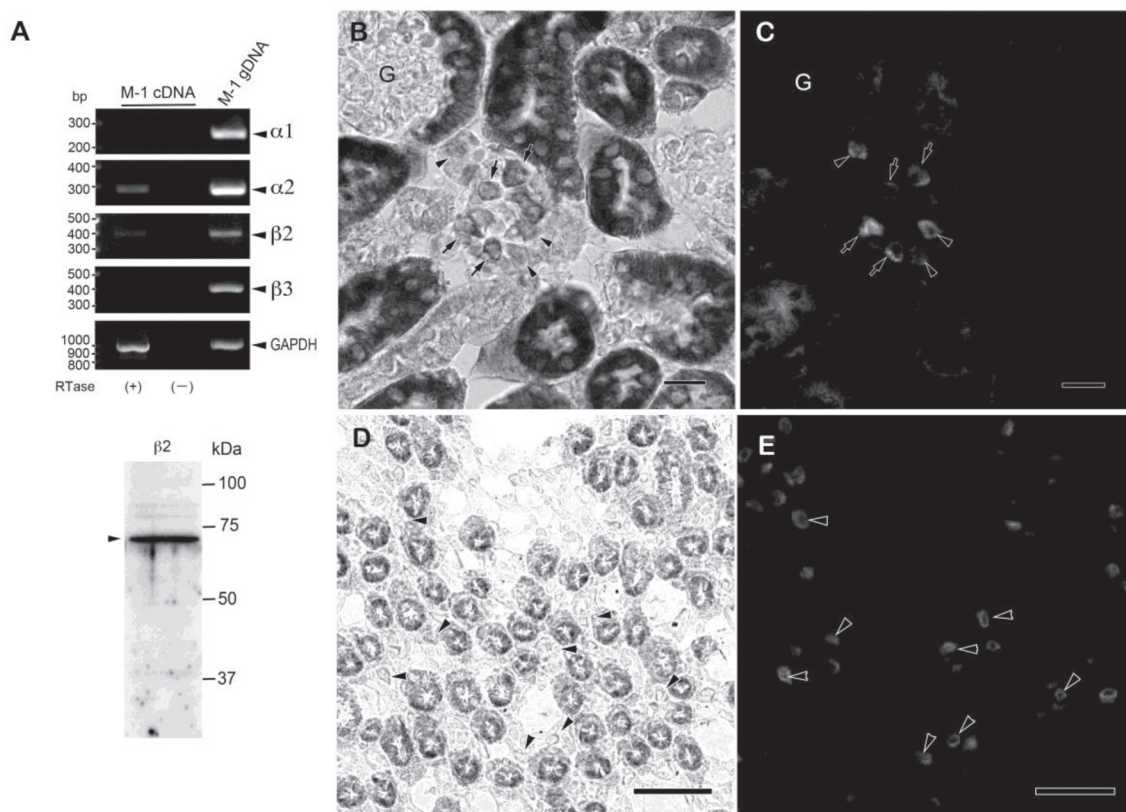


Fig. 2. Expression of adrenergic receptors in M-1 cells and histological localization of the $\beta 2$ receptor in the mouse kidney. A) RT-PCR (upper column) of ADRs in M-1 total cellular RNA (cDNA, lane 1) and genomic DNA (gDNA, lane 3). The $\alpha 2$ (second row) and $\beta 2$ (third row) ADRs were amplified from M-1 total cellular RNA, but the $\alpha 1$ (first row) and $\beta 3$ (fourth row) ADRs were not. No positive band was observed in RTase (-) negative control lane (lane 2). Immunoblot of the $\beta 2$ receptor (lower column) shows a specific 60–75 kDa band (arrowhead). B) and C) Immunohistochemistry of the $\beta 2$ receptor (B) and AQP6 (C) in the mouse renal cortex (arrows indicate the same points on both images). Arrows indicate AQP6-positive, $\beta 2$ -positive cells, and arrowheads indicate AQP6-positive, $\beta 2$ -negative cells in the CCDs. D) and E) Immunohistochemistry of the $\beta 2$ receptor (D) and AQP6 (E) in the outer medulla. $\beta 2$ receptor immunoreactivities were observed to the straight segment of proximal tubules, but not in the collecting ducts. Arrowheads (AQP6 positive cells) indicate the same points on both images. G: glomerulus. Bar=20 μm (B and C) and 100 μm (D and E).

tions were then washed with 50 mM Tris-HCl (pH 7.6) and incubated with DAB-Ni for 10 min. The control experiment was performed by omitting acetylthiocholine iodide from the reaction buffer. Double-labeling histochemistry was carried out with anti-AQP6 antibodies for cell type identification.

RESULTS

To determine whether the M-1 cell line expresses renal ICC markers, RT-PCR was performed on total RNA isolated from M-1 cells and from normal murine kidney. AQP6, which is specifically expressed by ICCs in the mammalian kidney, was amplified from total RNA isolated from M-1 cells. Further, immunoblotting of protein isolated from M-1 cells revealed the typical AQP6 banding pattern [50], consisting of a low molecular weight monomeric band and a high molecular weight glycosylated band (Fig. 1A). In contrast, AQP2, which is specifically expressed in collecting

duct principal cells, was amplified at high levels in total RNA isolated from murine renal tissue, but at very low levels in total RNA isolated from M-1 cells (Fig. 1B). Immunoblotting analysis revealed the typical AQP2 banding pattern [1], consisting of a low molecular weight monomeric band and a high molecular weight glycosylated band, in protein isolated from murine renal cell membranes, but not from M-1 cell membranes (Fig. 1B). These banding patterns were not seen in control experiments in which the primary antibodies were either omitted or incubated with blocking peptides. Immunofluorescence of cultured cells showed the AQP6 positive, but the AQP2 negative (Fig. 1). These findings indicate that the expression patterns of M-1 cells are more similar to ICCs than to principal cells.

Neurotransmitter receptor expression ($\alpha 1$, $\alpha 2$, $\beta 2$ and $\beta 3$ ADRs and m1, m3, m4 and m5 mAChRs) in M-1 cells was examined by RT-PCR. Because ADR $\beta 1$ and mAChR m2 were not expressed in the mouse kidney (data not shown),

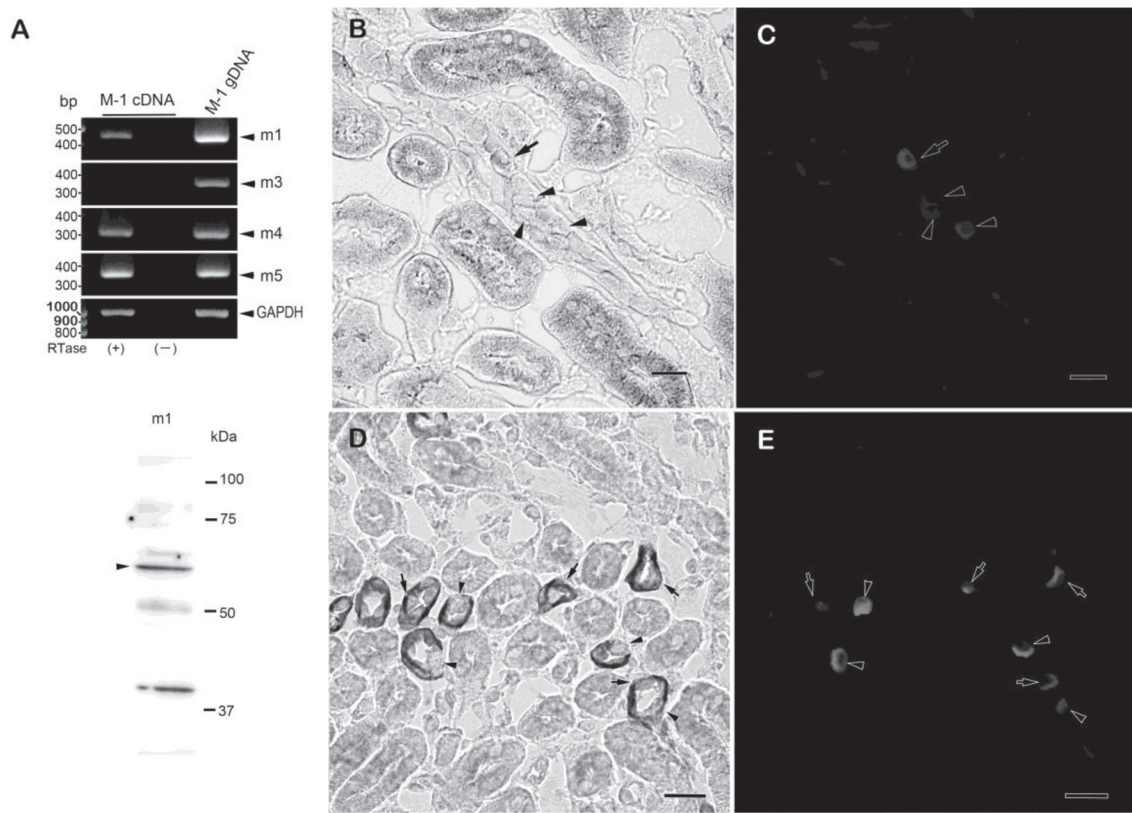


Fig. 3. Expression of mAChRs in M-1 cells and immunohistochemical localization of the m1 ADR in the mouse kidney. A) RT-PCR (upper column) of m1, m3, m4 and m5 receptor subtypes in M-1 total cellular RNA (lane 1, arrowheads). Genomic DNA was used as a control (lane 3). No positive band was observed in RTase (–) negative control lane (lane 2). Immunoblot (lower column) demonstrating the presence of the m1 receptor subtype in the M-1 total membrane protein fraction. The most intense band is observed at 55 to 70 kDa (arrowhead). B) to E) Immunohistochemistry demonstrating the presence of the m1 mAChR (B and D) and AQP6 (C and E) in the cortex (B and C) and renal outer medulla (D and E). Arrows indicate AQP6-positive, m1-positive cells. Arrowheads indicate AQP6-positive, m1-negative cells. Reactions of m1 antibody were stronger to the medullary collecting ducts (B) than to the CCDs (D). Bar=20 μ m.

they were excluded from this study. The $\alpha 2$ and $\beta 2$ ADR subtypes were amplified from total RNA isolated from M-1 cells (Fig. 2A). When expression levels were normalized to genomic DNA amplification, the $\beta 2$ subtype was expressed at higher levels than the $\alpha 2$ subtype. Further, expression of the $\beta 2$ receptor protein was observed in membrane proteins isolated from M-1 cells (Fig. 2A). The $\alpha 2$ receptor subtype was not by immunoblot in M-1 cells (data not shown). No expression of the $\alpha 1$ or $\beta 3$ ADR subtypes was observed in mRNA isolated from M-1 cells.

We observed $\beta 2$ ADR immunoreactivity in proximal tubules and in cortical collecting ducts (CCDs) within the renal cortex (Fig. 2B). We found that, in the CCDs, $\beta 2$ receptor-positive cells were also positive for AQP6 (Fig. 2C). However, several AQP6-positive ICCs did not demonstrate $\beta 2$ receptor expression. In the renal medulla, neither outer nor inner medullary collecting ducts demonstrated $\beta 2$ receptor expression (Fig. 2D and 2E). These findings suggest that two types of ICCs exist in the CCDs: those that do or do not express the $\beta 2$ ADR.

Examination of the expression of mAChRs in M-1 cells by RT-PCR revealed that the m1, m4 and m5 mAChRs are expressed by M-1 cells, but the m3 subtype is only expressed at a very low level (Fig. 3). Immunoblot analysis revealed that the m1 subtype was located in the membrane fraction of M-1 cellular proteins (Fig. 3A). Immunoblot analysis did not detect the m4 and m5 subtypes, despite several attempts with multiple antibodies. Immunohistochemical analysis of the m1 subtype revealed localization to the CCDs and to the outer and inner medullary collecting ducts (Fig. 3D). The m1 subtype was observed in almost all collecting duct cells, suggesting that it is expressed by both principal cells and ICCs. Reactivity was stronger in medullary cells than in cortical cells (Fig. 3B). Secondary staining with the AQP6 antibody, which identifies ICCs, showed that AQP6-positive cells throughout the collecting ducts were also m1-positive (Fig. 3B to 3E). However, several m1-negative ICCs were also observed in the collecting ducts. These findings indicate that principal cells and ICCs in the collecting ducts express the m1 receptor and provide further evidence that two types

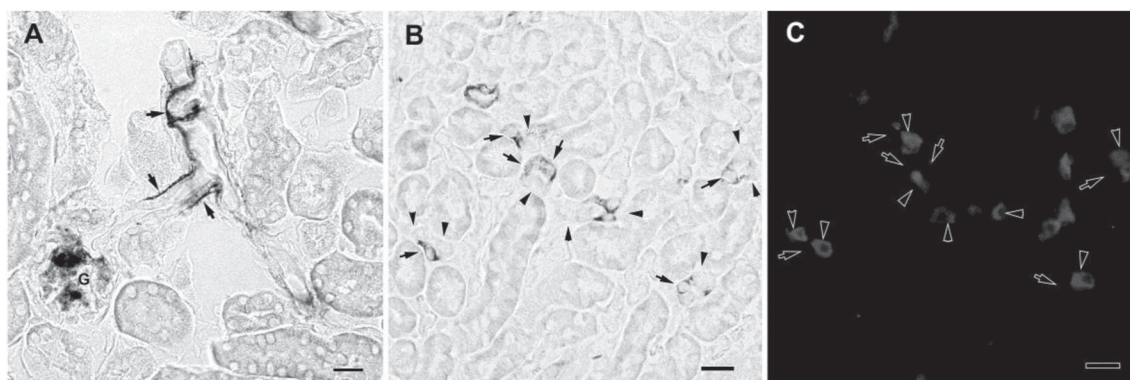


Fig. 4. Dual staining of AChE and AQP6 in CCDs. A) AChE was localized to the glomerulus (G) and the nerve fibers along the interlobular arterioles (arrows) B) AChE in CCD cells was stained with the modified Karnovsky-Roots method (arrows). C) AQP6 in the mouse renal cortex was stained by immunohistochemistry (arrowheads). AChE and AQP6 staining did not overlap in the CCDs. The arrows and arrowheads indicate identical cells in panels A and B. Bar=20 μ m.

of ICCs may exist, namely, those that do or do not express the m1 mAChR.

Double-labeling histochemistry using the modified Karnovsky-Roots method demonstrated localization of AChE to the glomeruli, the arterioles, the nerve fibers along the interlobular artery and the collecting ducts (Fig. 4A and 4B). In the collecting ducts, AChE was observed in the cortex and the outer medulla, but not in the inner medulla. Both AChE-positive and AChE-negative cells were scattered throughout these regions. AChE-positive cells did not stain with the AQP6 antibody (Fig. 4B and 4C), suggesting that they may be principal cells.

DISCUSSION

In this study, we examined the expression and localization of neurotransmitter receptors in the ICCs of the murine renal collecting ducts and in the murine renal epithelial M-1 cell line. RT-PCR and immunoblot analysis revealed that AQP6, but not AQP2, mRNA and protein are expressed in M-1 cells. As a control, we confirmed that both AQP6 and AQP2 can be amplified from M-1 genomic DNA, indicating that AQP2 is not defragmented in M-1 cellular DNA. These findings suggest that M-1 cells demonstrate ICC-like properties *in vitro*.

We identified both adrenergic and cholinergic receptor expression in M-1 cells. Multiple ADR subtypes have been identified in the kidney [11]. Activation of the ADR α subtype leads to vascular smooth muscle contraction and proximal tubule reabsorption [8, 34]. Activation of the ADR α 2 subtype decreases cAMP in the distal tubules and collecting ducts, leading to AVP release [2, 31, 33]. In M-1 cells, the α 2 receptor subtype was detected by RT-PCR, but not by immunoblot. It is difficult to determine whether the α 2 receptor is activated in M-1 cells and ICCs. In contrast, β 2 ADR mRNA and protein were both detected in M-1 cells. In murine renal tissue, β 2 receptor immunoreactivity was localized to the proximal tubules and collecting ducts. We observed that β 2-positive cells in the collecting ducts were also AQP6-positive, indicating the intercalated cell type. We

observed no β 2 receptor immunoreactivity in the medullary collecting ducts, indicating that the β 2 ADR may only be expressed by the ICCs of CCDs. Noradrenergic nerve fibers generally originate from the sympathetic ganglia, then run along the renal artery and branch with the interlobular artery [3]. The interstitial space between the renal tubules and the renal vasculature is extremely narrow [19], and it has been difficult to determine whether nerve fibers in this space innervate tubular cells or vascular smooth muscle cells. We have identified neurotransmitter receptors on ICCs within CCDs, suggesting that these cells are responsive to neuronal signals and may thus be the targets of the previously observed innervation.

We identified multiple mAChR subtypes expressed by M-1 cells. We observed high levels of mRNA expression of the m1, m4 and m5 mAChRs and low levels of m3 receptor expression. As m2 receptor mRNA was not amplified from murine renal tissue, we did not examine the expression of this receptor in M-1 cells. The odd numbered mAChR subtypes are Gq receptors, and the even numbered subtypes are Gi receptors. It is well known that Gq and Gi receptors activate the phospholipase C and adenylate cyclase signaling cascades, respectively [47]. However, the function of these receptor subtypes in ICCs remains to be clarified. We observed expression of the m1 subtype in M-1 cells as well as in ICCs and principal cells throughout the murine renal cortex and medulla. This finding suggests that M-1 cells and ICCs may be influenced by the cholinergic system via the m1 receptor. The lack of mAChR-specific antibodies has made the detection of mAChRs in mammalian tissues technically difficult. Because of this, we were able to detect the m1 subtype using immunoblot and immunohistochemical techniques, but were unable to detect the m4 and m5 subtypes, despite multiple attempts with several antibodies. Hence, the full array of mAChRs expressed by ICCs in CCDs remains unclear, and the cholinergic effects on ICCs may be more complex than previously thought.

We also examined AChE expression within the mouse kidney. We found AChE expression in principal cells located

near AQP6-positive ICCs. The AChE enzyme catalyzes the degradation of ACh. We observed that the m1 mAChR subtype was expressed in cells of the collecting ducts, including ICCs. Our findings suggest that ACh levels within the kidney may be locally regulated by AChE from principal cells. It has previously been reported that AChE is expressed by multiple renal cell types, including cells in the glomeruli and afferent arterioles, as well as in nephrons and efferent nerve fibers [4, 39]. We identified AChE expression in murine glomeruli and nerve fibers, in addition to the collecting ducts. These findings indicate that ACh levels may be locally regulated within various renal tissues. The origin of renal ACh is unknown. The renal nerve plexus contains numerous efferent fibers, however, almost all of these fibers are adrenergic; neither vagal nor sacral nerve fibers innervate renal tissues [4, 12, 23, 29]. In our previous study, we found that some CCD principal cells in rats express choline acetyltransferase (ChAT), an enzyme that catalyzes the synthesis of ACh [22]. ChAT expression was unevenly distributed throughout the CCDs, suggesting localized expression. Another possible source of ACh is migrating cells from extrarenal tissues, such as lymphocytes [18, 48]. For example, T lymphocytes have been shown to express ChAT [17, 18, 45]. There is currently no evidence regarding the localization of ChAT-expressing T lymphocytes in renal tissue, but this may be one mechanism by which ACh is delivered to nephrons.

In conclusion, we showed that M-1 cellular expression of adrenergic and cholinergic receptors mimics that of mouse renal ICCs. To determine whether M-1 cells are useful for the study of the neuronal effects to the ICCs, further studies will be needed.

ACKNOWLEDGMENTS. The authors wish to thank Ms. M. Hatta and Mr. Gion (Hyogo College of Medicine) for their secretarial assistance. This study was supported in part by a Grant-In-Aid for Science Research (C), JSPS, KAKENHI (25460278).

REFERENCES

- Bai, L., Fushimi, K., Sasaki, S. and Marumo, F. 1996. Structure of aquaporin-2 vasopressin water channel. *J. Biol. Chem.* **271**: 5171–5176. [Medline] [CrossRef]
- Bankir, L., Bichet, D. G. and Bouby, N. 2010. Vasopressin V2 receptors, ENaC, and sodium reabsorption: a risk factor for hypertension? *Am. J. Physiol. Renal Physiol.* **299**: F917–F928. [Medline]
- Barajas, L., Liu, L. and Powers, K. 1992. Anatomy of the renal innervation: intrarenal aspects and ganglia of origin. *Can. J. Physiol. Pharmacol.* **70**: 735–749. [Medline]
- Barajas, L., Wang, P. and De Santis, S. 1976. Light and electron microscopic localization of acetylcholinesterase activity in the rat renal nerves. *Am. J. Anat.* **147**: 219–234. [Medline] [CrossRef]
- Barajas, L. and Wang, P. 1975. Demonstration of acetylcholinesterase in the adrenergic nerves of the renal glomerular arterioles. *J. Ultrastruct. Res.* **53**: 244–253. [Medline] [CrossRef]
- Barajas, L., Powers, K. and Wang, P. 1985. Innervation of the late distal nephron: an autoradiographic and ultrastructural study. *J. Ultrastruct. Res.* **92**: 146–157. [Medline] [CrossRef]
- Barajas, L. and Wang, P. 1983. Simultaneous ultrastructural visualization of acetylcholinesterase activity and tritiated norepinephrine uptake in renal nerves. *Anat. Rec.* **205**: 185–195. [Medline] [CrossRef]
- Bello-Reuss, E. 1980. Effect of catecholamines on fluid reabsorption by the isolated proximal convoluted tubule. *Am. J. Physiol.* **238**: F347–F352. [Medline]
- Fadem, S. Z., Hernandez-Llamas, G., Patak, R. V., Rosenblatt, S. G., Lifschitz, M. D. and Stein, J. H. 1982. Studies on the mechanism of sodium excretion during drug-induced vasodilatation in the dog. *J. Clin. Invest.* **69**: 604–610. [Medline] [CrossRef]
- Fonteles, M. C. and Karow, A. M. Jr. 1975. Isolated kidney preservation in relationship to cholinergic and adrenergic processes. *Surg. Gynecol. Obstet.* **141**: 267–276. [Medline]
- Garg, L. C. 1992. Actions of adrenergic and cholinergic drugs on renal tubular cells. *Pharmacol. Rev.* **44**: 81–102. [Medline]
- Gattone, V. H. 2nd., Marfurt, C. F. and Dallie, S. 1986. Extrinsic innervation of the rat kidney: a retrograde tracing study. *Am. J. Physiol.* **250**: F189–F196. [Medline]
- Goldsmith, D. J., Covic, A. C., Venning, M. C. and Ackrill, P. 1997. Ambulatory blood pressure monitoring in renal dialysis and transplant patients. *Am. J. Kidney Dis.* **29**: 593–600. [Medline] [CrossRef]
- Hamm, L. L., Alpern, R. J. and Preisig, P. A. 2013. Cellular mechanisms of renal tubular acidification. pp. 1917–1978. In Seidin and Giebisch's *The Kidney*, 5th ed. (Alpern, R. J., Caplan, M. J. and Moe, O. W. eds.), Elsevier, Amsterdam.
- Johns, J. E. and Kopp, U. C. 2012. Neural control of renal function. pp. 451–486. In Seidin and Giebisch's *The Kidney*, 5th ed. (Alpern, R. J., Caplan, M. J. and Moe, O. W. eds.), Elsevier, Amsterdam.
- Kanai, T. and Krum, H. 2013. New treatment for old disease: management of resistant hypertension by percutaneous renal sympathetic denervation. *Rev. Esp. Cardiol. (Engl. Ed.)* **66**: 734–740. [Medline] [CrossRef]
- Kawashima, K., Fujii, T., Moriwaki, Y., Misawa, H. and Horiguchi, K. 2012. Reconciling neuronally and nonneuronally derived acetylcholine in the regulation of immune function. *Ann. N. Y. Acad. Sci.* **1261**: 7–17. [Medline] [CrossRef]
- Kawashima, K. and Fujii, T. 2004. Expression of non-neuronal acetylcholine in lymphocytes and its contribution to the regulation of immune function. *Front. Biosci.* **9**: 2063–2085. [Medline] [CrossRef]
- Kriz, W. and Kaissling, B. 2013. Structural organization of the mammalian kidney. pp. 595–691. In: Seidin and Giebisch's *The Kidney*, 5th ed. (Alpern, R. J., Caplan, M. J. and Moe, O. W. eds.), Elsevier, Amsterdam.
- Lipkin, G. W., Tucker, B., Giles, M. and Raine, A. E. 1993. Ambulatory blood pressure and left ventricular mass in cyclosporin- and non-cyclosporin-treated renal transplant recipients. *J. Hypertens.* **11**: 439–442. [Medline] [CrossRef]
- Liu, F. and Gesek, F. A. 2001. α_1 -Adrenergic receptors activate NHE1 and NHE3 through distinct signaling pathways in epithelial cells. *Am. J. Physiol. Renal Physiol.* **280**: F415–F425. [Medline]
- Maeda, S., Jun, J.G., Kuwahara-Otani, S., Tanaka, K., Hayakawa, T. and Seki, M. 2011. Non-neuronal expression of choline acetyltransferase in the rat kidney. *Life Sci.* **89**: 408–414. [Medline] [CrossRef]
- Maeda, S., Kuwahara-Otani, S., Tanaka, K., Hayakawa, T. and Seki, M. 2014. Origin of efferent fibers of the renal plexus in the rat autonomic nervous system. *J. Vet. Med. Sci.* **76**: 763–765. [Medline] [CrossRef]
- McArdle, S., Garg, L. C. and Crews, F. T. 1988. Cholinergic

- stimulation of phosphoinositide hydrolysis in rabbit kidney. *J. Pharmacol. Exp. Ther.* **244**: 586–591. [Medline]
25. McArdle, S. and Garg, L. C. 1989. Cholinergic stimulation of phosphoinositide hydrolysis in renal medullary collecting duct cells. *J. Pharmacol. Exp. Ther.* **248**: 682–686. [Medline]
 26. Müller, J. and Barajas, L. 1972. Electron microscopic and histochemical evidence for a tubular innervation in the renal cortex of the monkey. *J. Ultrastruct. Res.* **41**: 533–549. [Medline] [CrossRef]
 27. Nielsen, S., Frokiaer, J., Marples, D., Kwon, T. H., Agre, P. and Knepper, M. A. 2002. Aquaporins in the kidney: from molecules to medicine. *Physiol. Rev.* **82**: 205–244. [Medline]
 28. Nitschke, R., Henger, A., Ricken, S., Müller, V., Kottgen, M., Bek, M. and Pavenstadt, H. 2001. Acetylcholine increases the free intracellular calcium concentration in podocytes in intact rat glomeruli via muscarinic M₅ receptors. *J. Am. Soc. Nephrol.* **12**: 678–687. [Medline]
 29. Norvell, J. E. and Anderson, J. M. 1983. Assessment of possible parasympathetic innervation of the kidney. *J. Auton. Nerv. Syst.* **8**: 291–294. [Medline] [CrossRef]
 30. Ohshiro, K., Yaoita, E., Yoshida, Y., Fujinaka, H., Matsuki, A., Kamiie, J., Kovalenko, P. and Yamamoto, T. 2001. Expression and immunolocalization of AQP6 in intercalated cells of the rat kidney collecting duct. *Arch. Histol. Cytol.* **64**: 329–338. [Medline] [CrossRef]
 31. Pettinger, W. A., Umemura, S., Smyth, D. D. and Jeffries, W. B. 1987. Renal alpha 2-adrenoceptors and the adenylate cyclase-cAMP system: biochemical and physiological interactions. *Am. J. Physiol.* **252**: F199–F208. [Medline]
 32. Robey, R. B., Ruiz, O. S., Baniqued, J., Mahmud, D., Espiritu, D. J., Bernardo, A. A. and Arruda, J. A. 2001. SFKs, Ras, and the classic MAPK pathway couple muscarinic receptor activation to increased Na-HCO₃ cotransport activity in renal epithelial cells. *Am. J. Physiol. Renal Physiol.* **280**: F844–F850. [Medline]
 33. Rouch, A. J. and Kudo, L. H. 2002. Agmatine inhibits arginine vasopressin-stimulated urea transport in the rat inner medullary collecting duct. *Kidney Int.* **62**: 2101–2108. [Medline] [CrossRef]
 34. Rouse, D., Williams, S. and Suki, W. N. 1990. Clonidine inhibits fluid absorption in the rabbit proximal convoluted renal tubule. *Kidney Int.* **38**: 80–85. [Medline] [CrossRef]
 35. Ruiz, O. S., Qiu, Y. Y., Cardoso, L. R. and Arruda, J. A. 1997. Regulation of the renal Na-HCO₃ cotransporter: VII. Mechanism of the cholinergic stimulation. *Kidney Int.* **51**: 1069–1077. [Medline] [CrossRef]
 36. Santipillai, G. R. and Ferro, A. 2014. Renal denervation as an option for the management of hypertension. *J. Biomed. Res.* **28**: 18–24. [Medline] [CrossRef]
 37. Stoos, B. A., Naray-Fejes-Toth, A., Carretero, O. A., Ito, S. and Fejes-Toth, G. 1991. Characterization of a mouse cortical collecting duct cell line. *Kidney Int.* **39**: 1168–1175. [Medline] [CrossRef]
 38. Strait, K. A., Stricklett, P. K., Chapman, M. and Kohan, D. E. 2010. Characterization of vasopressin-responsive collecting duct adenylyl cyclases in the mouse. *Am. J. Physiol. Renal Physiol.* **298**: F859–F867. [Medline]
 39. Suda, A. 1986. A histochemical localization of acetylcholinesterase and cholinesterase activities in mammalian kidneys. *Acta Histochem.* **79**: 107–114. [Medline] [CrossRef]
 40. Summers, R. J., Broxton, N., Hutchinson, D. S. and Evans, B. A. 2004. The Janus faces of adrenoceptors: factors controlling the coupling of adrenoceptors to multiple signal transduction pathways. *Clin. Exp. Pharmacol. Physiol.* **31**: 822–827. [Medline] [CrossRef]
 41. Sundaresan, P. R., Fortin, T. L. and Kelvie, S. L. 1987. Alpha- and beta-adrenergic receptors in proximal tubules of rat kidney. *Am. J. Physiol.* **253**: F848–F856. [Medline]
 42. Szénási, G., Bencsath, P. and Takacs, L. 1985. Proximal tubular transport and urinary excretion of sodium after renal denervation in sodium depleted rats. *Pflugers Arch.* **403**: 146–150. [Medline] [CrossRef]
 43. Takata, K., Matsuzaki, T. and Tajika, Y. 2004. Aquaporins: water channel proteins of the cell membrane. *Prog. Histochem. Cytochem.* **39**: 1–83. [Medline] [CrossRef]
 44. Thorp, A. A., Larsen, R. N. and Schlaich, M. P. 2013. Renal sympathetic nerve ablation for the management of resistant hypertension: an update. *Curr. Opin. Nephrol. Hypertens.* **22**: 607–614. [Medline] [CrossRef]
 45. Tsuji, S. and Larabi, Y. 1983. A modification of thiocholine-ferricyanide method of Karnovsky and Roots for localization of acetylcholinesterase activity without interference by Koelle's copper thiocholine iodide precipitate. *Histochemistry* **78**: 317–323. [Medline] [CrossRef]
 46. Vander, A. J. 1964. Effects of acetylcholine, atropine, and physostigmine on renal function in the dog. *Am. J. Physiol.* **206**: 492–498. [Medline]
 47. Wess, J., Blin, N., Mutschler, E. and Bluml, K. 1995. Muscarinic acetylcholine receptors: structural basis of ligand binding and G protein coupling. *Life Sci.* **56**: 915–922. [Medline] [CrossRef]
 48. Wessler, I. and Kirkpatrick, C. J. 2008. Acetylcholine beyond neurons: the non-neuronal cholinergic system in humans. *Br. J. Pharmacol.* **154**: 1558–1571. [Medline]
 49. Yasui, M., Hazama, A., Kwon, T. H., Nielsen, S., Guggino, W. B. and Agre, P. 1999. Rapid gating and anion permeability of an intracellular aquaporin. *Nature* **402**: 184–187. [Medline] [CrossRef]
 50. Yasui, M., Kwon, T. H., Knepper, M. A., Nielsen, S. and Agre, P. 1999. Aquaporin-6: An intracellular vesicle water channel protein in renal epithelia. *Proc. Natl. Acad. Sci. U.S.A.* **96**: 5808–5813. [Medline] [CrossRef]